27th EPS Conference on Contr. Fusion and Plasma Phys. Budapest, 12-16 June 2000 ECA Vol. **24B** (2000) 225 -228

Investigation of the influence of edge parameters on L-H-mode transitions on COMPASS-D

H. Meyer, P. G. Carolan, N. J. Conway, A. R. Field, S. J. Fielding, P. Helander and P. B. Jones[†]

EURATOM/UKAEA Fusion Association, Culham Science Centre, Abingdon, Oxfordshire, OX14 3DB, UK

[†]Department of Physics, Imperial College of Science and Technology & Medicine, Prince Consort Road, London, SW7 2BZ, UK

1 Introduction

The transition of a magnetically confined plasma from L-mode to H-mode is still not well understood. Although many theories have been developed in recent years [1] none of them is completely satisfactory. In particular the influence of neutral particles and the causality of events are controversial subjects. It is widely believed that a sheared perpendicular electric field and the associated sheared poloidal (and toroidal) plasma flows observed in the H-mode phase account for the reduction of turbulent cross field transport. However due to the lack of detailed experimental data many problems still remain unsolved. To obtain good experimental data a fast time resolution is required because of the fast time scales associated with ELMs or an abrupt L/H transition as well as spatial profiles of the main plasma parameters such as electron density n_e, electron temperature T_e, ion temperature T_i, poloidal velocity $v_{i\theta}$, toroidal velocity $v_{i\phi}$, and neutral (atomic) density n_{D}.

Most of the above parameters have been measured in recent experiments on COMPASS-D using a combined diagnostic consisting of a thermal helium beam diagnostic (HELIOS) [2] and a high resolution spectrometer (CELESTE) [3]. Both diagnostics observe the same spatial region at the plasma boundary with shared optics. To investigate the evolution of the plasma edge profiles during L/H-transitions ELM-free H-modes were generated in ohmic SND discharges by shutting off the gas fuelling. Within this ELM-free phase a stepped gas puff was applied to trigger a transition back into L-mode followed by a subsequent second L/H transition.

2 Diagnostic

The evolution of the radial profiles of T_e, n_e, n_{D}, $v_{z\theta}$, T_z, and the relative impurity density $\tilde{n}_z$ was measured on COMPASS-D ($R = 0.56$ m, $a = 0.17$ m) using the recently implemented novel HELIOS/CELESTE diagnostic observing the plasma boundary at the outboard mid-plane. HELIOS is a thermal helium beam diagnostic providing $n_e(r)$, $T_e(r)$ from HeI line ratios and the absolute D_α-intensity on 10 spatial points with a time resolution of $\Delta t = 2$ ms $\rightarrow 5$ ms. CELESTE is a multi-chord Doppler-spectrometer delivering $I_z(r)$, $v_{z\theta}(r)$, and $T_z(r)$ for the chosen impurity Z (19 chords, $\Delta t = 1$ ms $\rightarrow 2.5$ ms). For the experiments here CELESTE recorded the HeII resonance line emission at $\lambda_0 = 468.67$ nm. HeII is locally produced by the thermal helium beam ($\lambda_{\mathrm{ion}}(0 \rightarrow 1^+) \approx 3$ mm). These ions are further ionized after $\lambda_{\mathrm{ion}}(1^+ \rightarrow 2^+) \approx 3$ m which is smaller than the toroidal perimeter $2\pi R \approx 4.6$ m on COMPASS-D. Hence, the HeII emission detected is essentially localized to the beam. The neutral density profile n_{D} was deduced from the absolutely calibrated D_α-intensity. Since the intensity is a line integrated quantity the measured profile has to be inverted to obtain radial profiles of the emissivity. The information provided by HELIOS is not sufficient for a full tomographic reconstruction. However, assuming that D_α-emissivity is constant on flux surfaces in the region of interest the radial profile of n_{D} can be calculated using a maximum entropy fit [4] for the D_α inversion and applying a collisional radiative model to the inverted profiles [5].

3 Shot preparation

Figure 1 shows time traces for the shots 28443 (red; without gas puff), and 28447 (black; with gas puff) of (a) plasma current I_P, (b) line averaged density $\bar{n}_e$, (c) averaged D_α-intensity through the X-Point, and (d) the driving voltage of the piezo valve U_{Piezo} controlling the inlet of deuterium. The sudden drop of the D_α-intensity at $t \approx 0.16$ s (trace b) indicates the transition to an ELM-free H-mode 3 ms after termination of the gas fuelling. In ohmic discharges on COMPASS-D usually a gradual transition between L-mode and ELM-free H-mode through a "dithering" ELMy phase is observed and the D_α traces (c) show type III ELMs before the ELM-free phase. However, as indicated by the detail in Fig. 1 the plasma is close or even in full L-mode just before the transition, due to the sustained fuelling and the increasing density. In shot 28447 a stepped gas puff was applied at $t_3 = 0.18$ s (trace d). The bigger first-part ($\Delta t = 10$ ms) triggers an H-L-transition which then is sustained by the slightly smaller second-part ($\Delta t = 10$ ms). After the gas is shut-off the plasma enters again into an ELM-free H-mode.

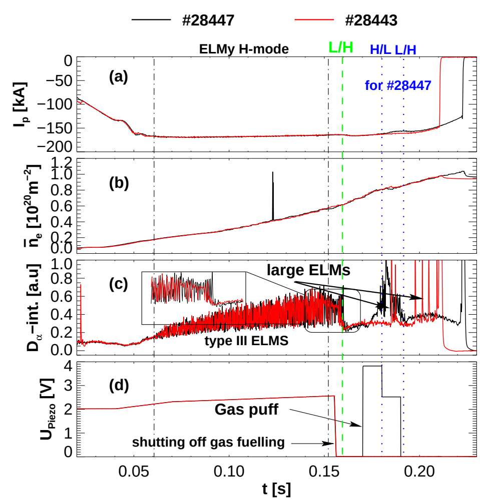

Figure 1: *Time traces for the COMPASS-D shot no. 28447 and 28443 of relevant machine parameters (see text).*

4 Results

Parameters are analysed using flux-coordinates (ψ, θ, ϕ) [6], with $\psi = \Psi_p/2\pi$ being the poloidal flux function calculated with the equilibrium code EFIT [7], θ the usual poloidal angle and ϕ the toroidal angle defined in the opposite direction to the toroidal angle in the cylindrical machine coordinate system (R, φ, Z).

Fig. 2 shows time traces of the poloidal velocity along surfaces of constant normalized flux $\psi_N = (\psi - \psi_0)/(\psi_S - \psi_0)$ where ψ_0, and ψ_S denote the flux on the magnetic axis and the separatrix respectively. To illustrate the different phases of the shot the D_α-intensity and U_{Piezo} are also depicted. Note, that the time points are chosen to be at the end of the integration interval to avoid confusion with the causality of events.

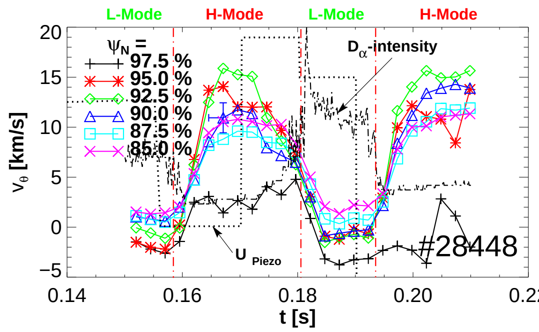

Figure 2: *Poloidal velocity on constant flux surfaces as a function of time.*

The most striking feature is that there is no evidence for change in velocity shear prior to the L-H transitions within the observed region. But, *after* the plasma has entered the H-mode a considerable shear develops. This can also be seen from Fig. 3 showing E_ψ. Nevertheless, the importance of the velocity shear becomes evident on the H/L-transition where the velocity shear starts to decrease coincident with the onset of the gas puff. The plasma undergoes the transition only when the shear has fallen to a low value. The HeII velocity can however differ substantially from the plasma ion velocity. A more fundamental quantity is the radial electric field $E_\psi = \mathbf{E} \cdot \nabla\psi/|\nabla\psi|$.

We derive the electric field from the momentum balance equation for the impurity species $\alpha =$ He II. Only the contributions from the Lorentz force $-\mathbf{v}_z \times \mathbf{B}$ and the pressure gradient $\nabla p_z/(Z_z e n_z)$ have to be considered since the other terms, normalized to the pressure gradient term, scale as follows: inertia $\propto M_z^2 \approx 0.04$, perpendicular viscosity $\propto M_z \rho_z / L_\perp \approx 0.07$, neutral friction $\propto M_z L_\perp / \lambda_{zn} \approx 3 \cdot 10^{-6}$, coulomb friction $\propto M_z L_\perp / \lambda_{zi} \approx 5 \cdot 10^{-5}$ where $M_z = v_{z\theta} / v_{\mathrm{zth}}$, ρ_z the Larmor radius, $L_\perp$ the typical pressure gradient length, and $\lambda_{\alpha\beta}$ the mean free path for collisions between particles of species α with β. The contribution arising from the toroidal velocity v_ϕ can be neglected. This is because on COMPASS-D the toroidal velocity is usually smaller than v_θ [8]. Hence, being weighted with $B_\theta / B_\phi \approx 0.1$ it is negligible. Therefore, the radial electric field can be reasonably approximated by

$$E_\psi = \frac{\nabla p_z \cdot \nabla \psi}{Z_z e n_z |\nabla \psi|} - v_{z\theta} B_\phi. \tag{1}$$

In the following we show contour plots of the evolution of analysed parameters from the example shot 28448. This shot was similar to shot 28447 apart from a longer triggered L-mode phase due to a higher second part of the gas puff. In Figures 4 to 6 the abscissa is $\sqrt{\psi_\mathrm{N}} \sim r/a$ and the vertical lines correspond to the 90%, 95%, and 100% (separatrix) flux surfaces as indicated. The horizontal lines mark the transition times as can be seen from the D_α-traces at the right edge of the graphs.

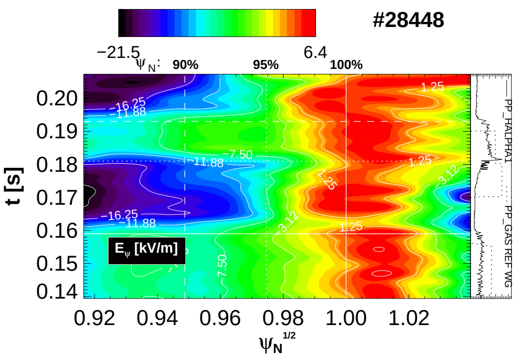

Figure 3: *Evolution of the radial electric field for shot 28448.*

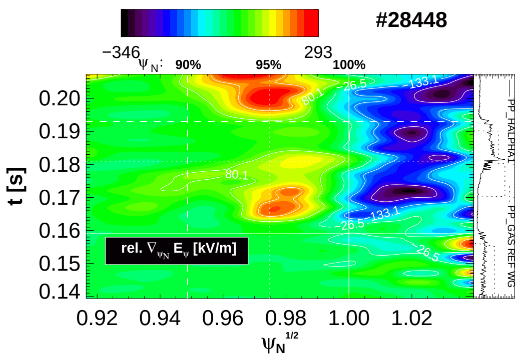

Figure 4: *Evolution of $\partial E_\psi / \partial \psi_\mathrm{N}$ relative to the shear during the first L-mode phase for shot 28448.*

The evolution of the electric field E_ψ is shown in Fig. 3. Within the confined region E_ψ points inwards with higher values in the H-mode phase and a maximum change of $\Delta E_\psi \approx -12\,\mathrm{kV/m}$. Although the velocity clearly has a maximum around the 92% flux surface (see Fig. 2) no minimum of E_ψ occurs.

The maximum shear in the electric field of $\partial E_\psi / \partial r \approx 2 \cdot 10^3\,\mathrm{kV/m^2}$ is around the 96% flux surface as can be seen from Fig. 4 showing the change of $\partial E / \partial \psi_\mathrm{N}$ with respect to the first L-mode phase. Note, that even in the L-mode phase the electric field already exhibits shear in this region. But, *after* the L/H-transition this shear increases. Correlated with the gas puff, the shear decreases *before* the H/L-transition.

Figures 5, and 6 show the evolution of n_e, and n_D respectively. As expected, the electron density inside the separatrix is higher in the H-mode than in L-mode. But, interestingly, the opposite is true outside the separatrix in the SOL. This is more pronounced in the triggered L-mode from $t = 0.18$ s to $t = 0.19$ s. The neutral density (Fig. 6) shows an opposite behaviour. Here, in L-mode the neutral density profile extends further into the plasma than in H-mode. However, the changes of the neutral density seem to follow the transition whereas the n_e-evolution is more correlated to the E_ψ-evolution. The fact that both electron and neutral density decrease at the separatrix suggests that the mean energy of the influx neutrals has decreased in H-mode compared to L-mode.

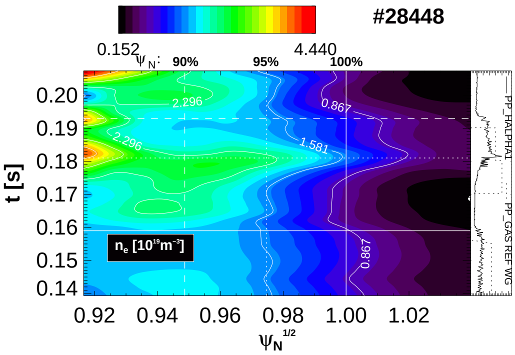

Figure 5: *Evolution of n_e for shot 28448.*

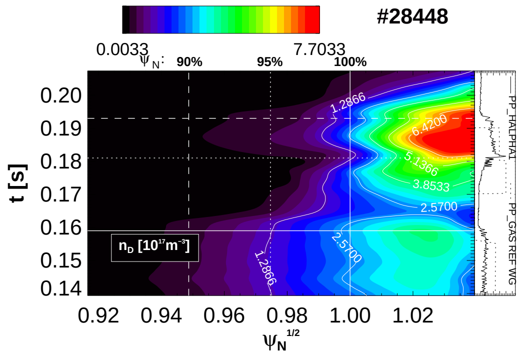

Figure 6: *Evolution of $n_{\rm D}$ for shot 28448.*

5 Conclusions

At this stage of the analysis no change in any of the analysed quantities was found prior to the transition into ELM-free H-mode. We find, however, that on COMPASS-D at least, the velocity and electric field shear build up around the 95% flux surface *only after* the L/H-transition. On the other hand the H/L-transition is preceded by a decay of the shear in this region corresponding to onset of the gas puff. Whether this decay is caused by a change in the local neutral density or not can not be deduced from our data. However, we regard this as unlikely since our data indicates that the evolution of $n_{\rm D}$ at the mid-plane *follows* the L/H and H/L-transition. The neutral density at the separatrix was found to be rather high $n_{\rm D} \approx 2.5 \cdot 10^{17}$ m^{-3} in L-mode and $n_{\rm D} \approx 1.7 \cdot 10^{17}$ m^{-3} in H-mode. The gradient lengths of both, $n_{\rm D}$ and n_e are shorter in H-mode than in L-mode and both quantities are reduced at the separatrix in H-mode suggesting that the mean energy of the influx neutrals is reduced in H-mode.

Acknowledgements

This work was jointly funded by the UK Department of Trade and Industry and EURATOM. The author H. Meyer is funded by a Marie Curie Research Training Grant.

References

[1] J. W. Connor and H. R. Wilson, Plasma Phys. Control. Fusion **42**, (2000).

[2] A. R. Field, P. G. Carolan, C. N. J., and O. M. G, Rev. Sci. Instr. **70**, 355 (1999).

[3] P. G. Carolan *et al.*, Rev.Sci.Inst. **68**, 1015 (1997).

[4] J. Skilling and S. Gull, Technical Report No. CUL 3130, Camebridge University. Dept. Applied Mathematics and Theoretical Physics (unpublished).

[5] K. Sawada, K. Eriguchi, and T. Fujimoto, J. Appl. Phys. **73**, 8122 (1993).

[6] R. D. Hazeltine and M. J. D., *Plasma Confinement*, Vol. 86 of *Frontiers of Physics* (Addison-Wesley Publishers, New York, 1992).

[7] L. L. Lao *et al.*, Nuclear Fusion **25**, 1611 (1985).

[8] P. G. Carolan *et al.*, in *22nd European Physical Society Conference on Controlled Fusion and Plasma Physics* (European Physical Society, Europhysics Letters, 27 Rue de la Vendée, POB 69, CH-1213 Petit Lancy 2, 1995), Vol. 21a, pp. 273–276.